CHAPTER 4

# Optical emissions from laser induced breakdown in external magnetic field

## 4.1. Introduction

The presence of a magnetic field during the expansion of laser induced plasma (LIP) may initiate several interesting phenomena, including conversion of plasma kinetic energy into thermal energy, emission enhancement, plasma instabilities and oscillations in the temporal history of emitting species. Plasma has a natural tendency to disperse, as the energetic particles that compose the plasma travel away from their initial positions at high velocity and the system of plasma will cease to exist. Plasma particles can be prevented from dispersion, with the aid of a magnetic field which acts on charged particles through Lorentz force. Magnetic fields can confine plasma, because the ions and electrons of which it consists will follow helical paths around the magnetic field lines. The dynamics of charged particles in magnetic field therefore forms an important area of investigation in the field of plasma physics.

A charged particle placed in a magnetic field will execute a circular orbit in the plane perpendicular to the direction of the field. We can also add an arbitrary drift along the direction of the magnetic field due to the Lorentz force $(q \cdot \mathrm{v} \times \mathrm{B})$ acting on the particle which depends only on the velocity component perpendicular to the magnetic field. The combination of these two motions gives a spiral trajectory to charged particle in magnetic field, with the field as the axis of the spiral. Thus, the freedom of motion in the perpendicular direction is thereby substantially suppressed by the field. If we pass to the limit of an extremely strong magnetic field, then the plasma behaves as if it were a one dimensional gas. These features are normally reflected in the properties of the collective modes in the plasma dynamics. The propagation characteristics of the electron plasma oscillation and the ion-acoustic wave are greatly altered by the magnetic field. Another notable feature is the periodicity brought about by the cyclotron motion of the particles. Plasma may thus exhibit new collective modes, propagating mainly in

directions perpendicular to the magnetic field, with a frequency near the fundamental or a higher harmonic frequency of the cyclotron motion [1].

The plasma plume will try to exclude the magnetic field as it expands. The magnetic gradient will then exert a backpressure against the expansion. The expansion will stop when the plasma energy is expended in doing work to oppose the magnetic gradient backpressure. The field may produce cross-field diffusion due to collision or parametric instabilities in the plasma.

In recent years, the use of a magnetic field to confine laser-induced plasmas has attracted more and more interest due to the strong coupling between magnetic field and the LIP.

## 4.2. Effect of magnetic field on laser induced plasma

The first set of experiments on the effects of magnetic fields on laser produced plasmas were made by Linlor et al [2,3]. He showed that the magnetic field was being displaced by the expanding conducting plasma. In 1969, Mattioli and Veron [4] observed that the intensity of recombination radiation was strongly reduced by the field. Haught et al [5] found that the stopping time of plasma in a magnetic field varies as $B^{-2/3}$. According to Tuckfield and Schwirzke [6], the field had very little effect on the early stages of development of plasma because, the kinetic pressure of the plasma then greatly exceeded the magnetic pressure. Sucov et al [7] studied LIP produced from aluminium targets in a transverse field. He observed narrowing of the plume and a five times increase in the duration of the luminosity of central core. There was a tendency for the plasma to break up in the field. The boundary moved across the magnetic field lines towards the laser almost as rapidly as it did with no field and this was the result of charge separation creating an electric field which cancelled out the v x *B* force.

In the following sections, we discuss the studies made on temporal emission profile of Lithium plasma in magnetic field.

## 4.3. Dynamics of LIP in magnetic field

When an external magnetic field is applied to LIP, the electrons and ions in the plasma are under the influence of Lorentz force, and the expansion and diffusion of the plasma are decelerated. From magnetohydrodynamic (MHD) equations, the parameter $\beta$ of the plasma is given by

$$\beta = \frac{8\pi\ nkT_e}{B^2} = \frac{particle\ \ pressure}{magnetic\ \ field\ \ pressure} \qquad (4.1)$$

This indicates the size of the diamagnetic effect [8] and is also called thermal $\beta$ of the plasma. The deceleration of the plasma expansion under the influence of a magnetic field is given as [9],

$$\frac{v_2}{v_1} = \left(1 - \frac{1}{\beta}\right)^{1/2} \tag{4.2}$$

where, $v_1$ and $v_2$ respectively are the asymptotic plasma expansion velocity in the absence and presence of the magnetic field. When $\beta$=1, the plasma would be stopped by the magnetic field. In the case of high $\beta$, the magnetic confinement would not be obvious while in the case of low $\beta$ plasma, the magnetic confinement would be effective. Considering an increase in plasma density under magnetic confinement, Rai et al derived a simple expression giving the ratio of plasma emission in the presence ($I_2$) as well as in the absence ($I_1$) of a magnetic field [9]:

$$\frac{I_2}{I_1} = \left(1 - \frac{1}{\beta}\right)^{-3/2} \left(\frac{t_1}{t_2}\right) \tag{4.3}$$

where, $t_1$ and $t_2$ are the emission times of plasma in the absence and presence of a magnetic field. This can explain the emission enhancement observed in some cases of plasma with $\beta$ values close to 1. At the same time, even with $\beta$ values close to 1, it is observed that the plume is not completely stopped by the field. This means that $\beta$ is not the only factor governing the nature of expansion.

After the initial conversion of thermal energy into the directed energy, the directed beta ($\beta_d$), given by,

$$\beta_d = \frac{4\pi\ n_e m v^2}{B^2} \tag{4.4}$$

becomes an important parameter. During the early phase of the plume expansion, $\beta_d$ is of the order of a few thousands which indicates that the plasma is in the regime of diamagnetic expansion [10]. The diamagnetic cavity (also called magnetic bubble) expands until the total excluded magnetic energy becomes comparable to the total plasma energy. By assuming that the plume expands spherically and considering that it is expanding from a flat surface into solid angle $2\pi$, the confinement radius ($R_b$) can be written as,

$$R_b = \left(\frac{3\mu_0 E_l}{\pi B^2}\right)^{1/3} \tag{4.5}$$

where $E_l$ is the total plasma energy and B is the applied magnetic field [11, 12].

It is found that $\beta_d$ varies by nearly three orders of magnitude during the plume expansion across the magnetic field. At earlier times, the charged particles diffuse through the

region occupied by the magnetic field and exclude the field. The diffusion coefficient of the charged particles perpendicular to a field is related to the field strength by [13],

$$D \propto \frac{1}{\beta^2 T^{1/2}} \tag{4.6}$$

So, an increase in temperature will reduce the diffusion across the magnetic field and eventually the plume will slow down considerably. At later times of plume evolution, the plasma cools and the magnetic field is able to diffuse across the boundary relatively fast. In this regime, $\beta_d$ approaches unity, indicating that the displaced magnetic field energy is approximately equal to the kinetic energy of the expanding plasma. The energy of the magnetic field is converted to heat within a characteristic magnetic diffusion time ($t_d$) given by,

$$t_d = \frac{4\pi\sigma R_b^{\,2}}{c^2} \tag{4.7}$$

where, $\sigma$ is the plasma conductivity which can be obtained with Spitzer formula [14].

## 4.4. Experimental setup

Lithium plasma is produced inside a multipurpose stainless steel chamber evacuated to a base pressure better than $10^{-5}$ mbar. The target used is pure solid lithium rod of 1.2 cm diameter and 5 cm length. A Q switched Nd: YAG laser with a repetition rate of 30 Hz and 8 ns FWHM is used to generate the plasma. The irradiance at the target is set to be about 2.23 GWcm$^{-2}$. A PMT with 2 ns rise time, mounted on the exit side of the monochromator has been used to record the signal. The output from the PMT is directly fed to a 500MHz digital oscilloscope (Tektronix, TDS 540). A pulsed transverse magnetic field is generated by discharging a high voltage capacitor bank through a pair of coaxial coils in Helmholtz configuration. During discharge, a high current flows through the coil and hence an induced magnetic field is obtained. The peak point of the magnetic pulse having $\cong$ 2ms life time is synchronized to the nanosecond laser pulse with the help of a programmed microcontroller.

A schematic diagram of the experimental setup is shown in figure 4.1. The diode lasers are helpful in the alignment of Nd:YAG beam on the target surface as well as in the proper imaging of different spatial slices of plasma on the spectrometer slit.. The

detailed description of the different components of the Helmholtz coil and capacitor bank circuit are given in the following sections:

### 4.4.1. Helmholtz coil

A Helmholtz coil is a pair of conducting circular coils each having *N* turns, carrying a current *I*, separated by a distance comparable to the radius of the circular loops. The arrangement produces a homogeneous magnetic field *B*, in the mid-plane between the two circular coils. The pair of inductor coils are made from copper wire of high current limit, wound on a perspex spool, each coil having 22 number of turns. The diameter of the coil is 0.5m and the distance between the pair of coils is 0.46m. Each of the coils is symmetrically fixed on either sides of the stainless steel vacuum chamber, in such a way that uniformity of the field is maintained at the center of the chamber. The axis of the coil and the plume expansion axis are mutually perpendicular. Both the coils are connected in parallel to the discharging circuit of the capacitor bank.

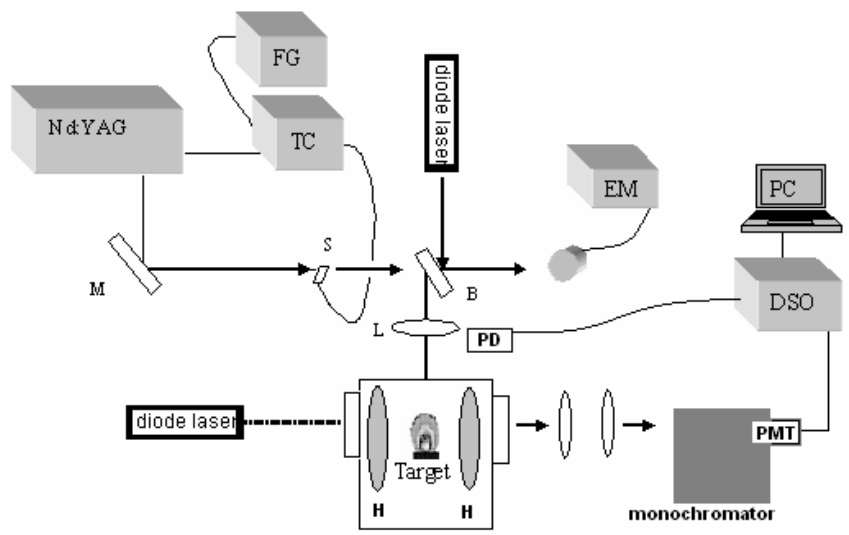


*Fig 4.1: Experimental setup used for the generation of plasma and optical spectroscopic studies. (FG- function generator, TC-timing controller, S-shutter, EM-energy meter, PD-photodiode, DSO-digital storage oscilloscope, PMT-photo multiplier tube, M-mirror, B-beam splitter, L-focusing lens, H-helmholtz coil).*

The magnetic field intensity at the center of the coil is calculated by the formula,

$$B = \frac{\mu_0 IR^2}{2(R^2 + x^2)^{3/2}} \tag{4.8}$$

where, $\mu_0 = 1.26 \times 10^{-6}$ Hm$^{-1}$, I is the current in amperes, $R$ is the coil radius in metre, $x$ is the distance between the centre of the chamber and each of the coil.

Since each coil consists of $N$ number of turns, $NI$ gives the total current in the coil.

so that, $$B = \frac{\mu_0 NIR^2}{2(R^2 + x^2)^{3/2}} \tag{4.9}$$

Since there are two such coils, we write,

$$B = \frac{\mu_0 NIR^2}{(R^2 + x^2)^{3/2}} \tag{4.10}$$

At $x = 0.23$ m,

$$B = 0.435 \times I \text{ (Gauss)} \tag{4.11}$$

Fig.4.2 shows the calibration curve for the field at the coil centre.

### 4.4.2. Rectifier circuit

The rectifier circuit shown in Fig 4.3 consists of a series-parallel combination of 19 numbers of 1 pF capacitors, IN-5408 diodes and 1 MΩ resistances. The circuit converts the ac input from a step-up transformer having a 1:20 turns ratio into a dc voltage, which is then used to charge the high voltage capacitor-bank up to the desired voltage. This voltage is then discharged using an ignitron switch to produce the pulsed magnetic field.

### 4.4.3. Capacitor bank

The rectifier circuit is connected to a 700μF/5kV high voltage capacitor through a 100 kΩ series resistance. The capacitor is connected to an ignitron switch, through the helmholtz coils. During the charging time of this high voltage capacitor, the ignitron switch is kept in an open state and the capacitor is thus disconnected from ground. At the discharging time, the ignitron switch is closed by giving a TTL trigger pulse and the capacitor discharges through the coil to the ground. The discharge of the capacitor will cause a high current flow through the coil and a pulsed magnetic field is produced around

the coil. The minimum charging time of the capacitor is 70 sec. Figures 4.4 and 4.5 show the capacitor-bank circuit and its firing circuit.

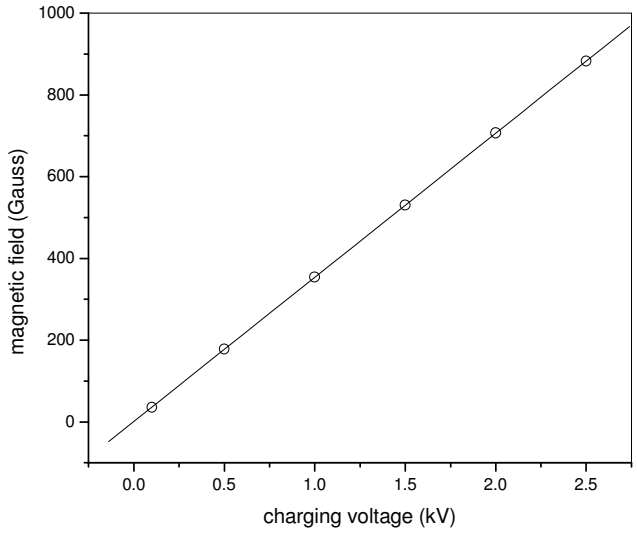


*Fig 4.2: The variation of magnetic field strength with capacitor voltage.*

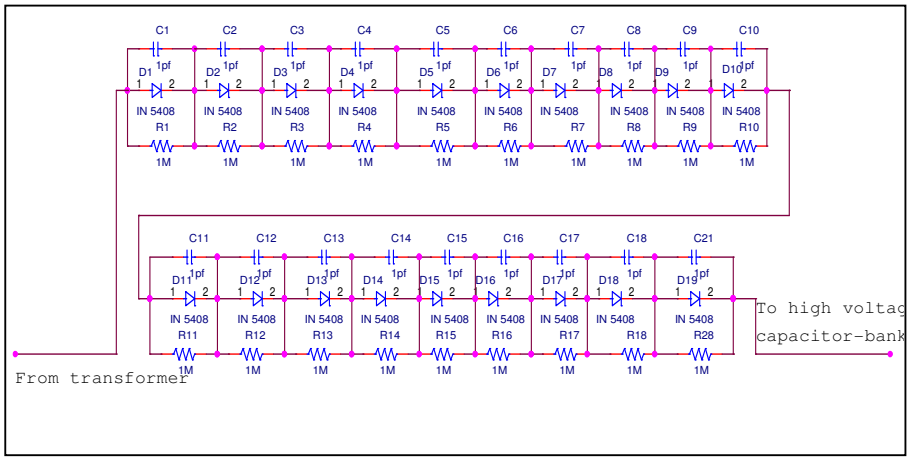


*Fig 4.3: The rectifier circuit.*

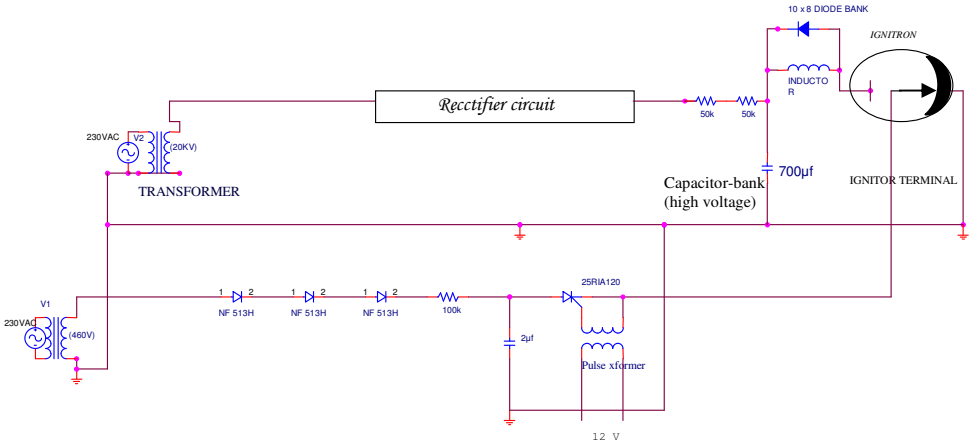


*Fig 4.4: The high voltage capacitor-bank circuit used for producing magnetic field.*

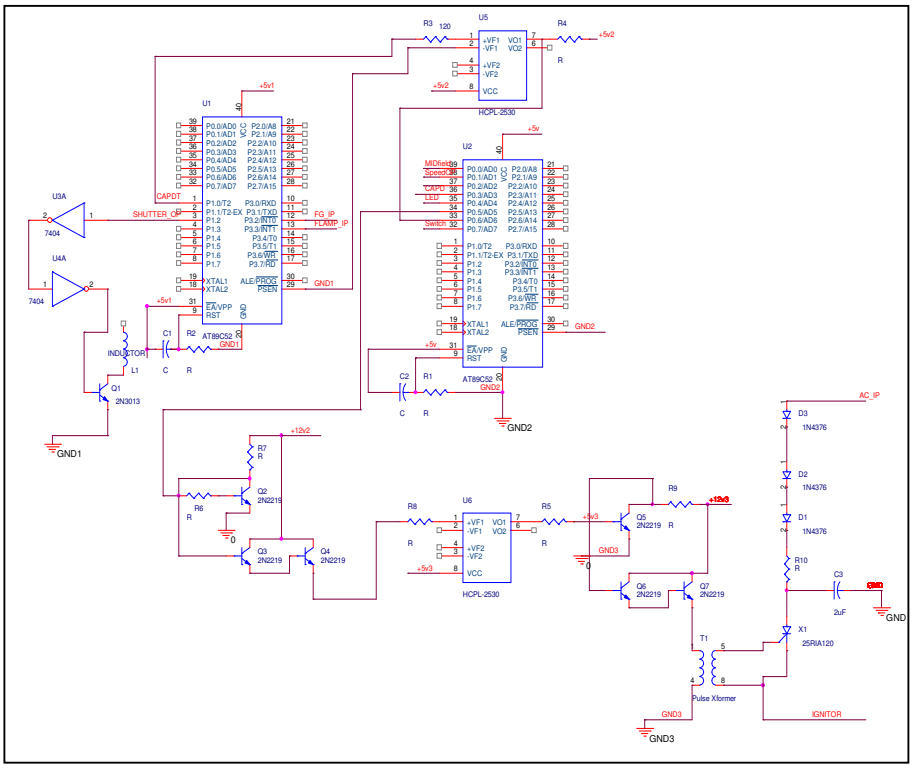


*Fig 4.5: firing circuit for the high voltage capacitor-bank*

### 4.4.4. Ignitron

The ignitron can be considered as a switch with an ingenious closing device of unusual reliability and almost indestructible electrodes. Without any applied voltage on the ignitor, the device is an open switch capable of reliably withstanding high voltages without conduction of current.

When a forward voltage is applied between the ignitron and the mercury-pool cathode, the resistance between the two elements decreases suddenly to a few ohms as a hot spot forms on the interface between the mercury surface and the ignitor. Mercury vapour is generated and a mercury glow discharge forms between the ignitor and the spot. This discharge is sustained by the electrical energy from the ignitor voltage source. While this condition exists, the presence of a forward voltage in excess of approximately 15 volts from anode to cathode will cause ionized mercury vapor to fill the tube and allow conduction to occur, making the ignitron a perfect closed switch. During conduction, the mercury pool cathode provides an almost unlimited supply of electrons making it an ideal switch for controlled capacitor discharges.

The change from nonconducting to conducting state of the ignitron is initiated by the ignitor excitation circuit. The ignitron requires a high voltage, which is provided by a Thyristor (25RIA-120).

### 4.4.5. Level converter circuit

The level converter circuit converts the small voltage (~12V) given by the transistor to about 315 V. This is supplied by a transformer and after rectification, this is transferred to the ignitor terminal to fire the capacitor-bank circuit. The level converter circuit consists of a series combination of three diodes (NF-513H) and a resistor (100 kΩ).

### 4.4.6. Micro-controller

A microcontroller (8051 architecture, chip no: 89C52) has been used to synchronize trigger pulses both from the flashlamp and the function generator so that maximum magnetic field can be obtained at the time of laser pulse. When the function generator trigger pulse and the flashlamp trigger pulse are given as inputs to the microcontroller it produces output triggers for the mechanical shutter and

also for the capacitor bank circuit. The shutter will open to receive one Q-switched laser pulse and closes just after the laser pulse. If delay adjustment is required for the capacitor bank circuit (for the synchronization of the laser pulse with the magnetic field pulse), then a second micro-controller can be programmed to produce the required delay for the output trigger from the first micro-controller.

### 4.4.7. Optocoupler

An optocoupler can be used to protect the system from the overvoltage damage, when the source and destination are at very different voltage levels. An optocoupler consists of an LED as a source of light and a phototransistor as the receiver. It transfers light signals from the LED to the phototransistor. This helps to transfer data between the circuit components, avoiding electrical contact between them.

### 4.4.8. Working

During manual triggering, a 50 MHz function generator provides a TTL trigger pulse to the synchronizing circuit. After synchronization, a 12 V TTL trigger will come to level converter circuit which then gets converted to 315 V and finally reaches the ignitor terminal. This closes the ignitron switch, which leads to the passage of current through the inductor coils in Helmholtz configuration and the desired pulsed magnetic field is generated around the coil.

### 4.4.9. Laser synchronization

When the flash lamp is triggered it will produce the laser output and simultaneously the capacitor bank circuit will be triggered to generate the magnetic field pulse. The pulse width and maximum amplitude of the magnetic field will be different from that of the laser pulse and they also differ in time. To fire the laser at the maximum field point, a microcontroller is programmed to produce a trigger pulse from the AND logic output of the flash lamp trigger pulse and the function generator trigger pulse so as to produce the required delay for both the shutter and the capacitor bank circuit. The trigger pulses for the laser and shutter operations are gated in such a way that the shutter is opened just before the laser pulse. The mechanical shutter opens only for one Q-switched laser pulse. Fig.4.6 shows the timing diagram for laser-synchronization.

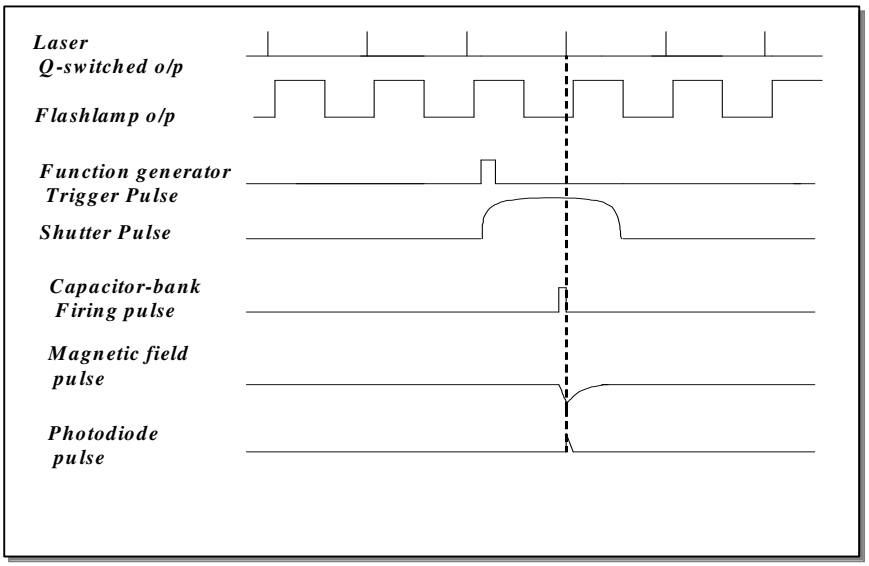


*Fig 4.6: Timing diagram showing the laser synchronization.*

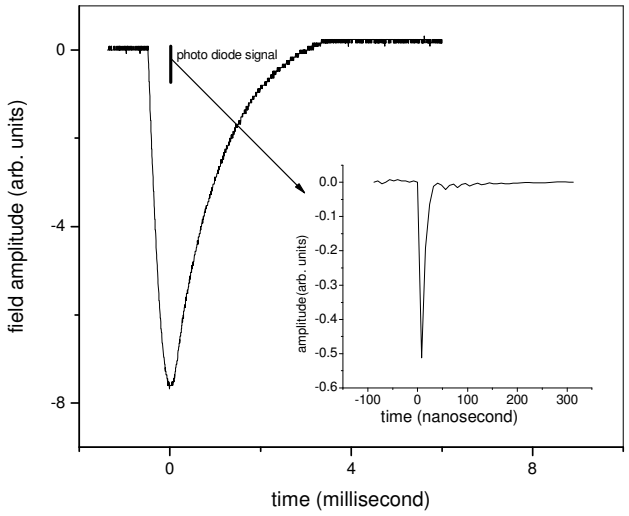


Fig 4.7: The magnetic field (ms) synchronized with the photodiode signal. A profile of the photodiode signal (ns) is given in the inset.

The magnetic pulse (millisecond range) and the photodiode signal (nanosecond range) are synchronized as shown in Fig.4.7 such that the photodiode signal comes at the maximum field point.

## 4.5. Discussion of results

Emission spectrum from the plasma is recorded using a the experimental setup of figure 4.1. Two neutral (6708Å from a $^2S$ - $^2P^0$ transition and 6103Å which is a $^2P^0$- 2D transition) lines and two ionic (4788Å from $^1P^0_1$ – $^1D_2$ transition and 5484Å which is a $^3S$ – $^3P^0$ transition) lines of Lithium are selected for the experiment and the field strengths has been varied between 100G and 800G. The plasma is allowed to expand in vacuum and in argon environment. The front region of the expanding plasma is not much affected by the applied field. Temporal profile investigations are therefore done on the slice of the plasma at 6 mm from the target surface.

### 4.5.1. Effect of magnetic field on intensity and time delay of plasma emissions in vacuum

In general, the line profiles of both the neutrals and ionic species show a gradual reduction of intensity with applied field (Fig.4.8 and Fig.4.9). The plasma density at 6mm is such that, the applied field is strong enough to penetrate the plasma. As seen in the figures, the intensity decrease with applied field is linear at 6mm.

As the particles in the expanding plasma propagate perpendicular to the applied magnetic field and when the field and plasma pressures are comparable, progressive development of a sharp boundary between the field and the plasma is possible. The expansion velocity of the plume normal to the target decreases and this reduces the forward spatial range of the particles. The slowing down of neutrals and ions in the presence of the field is consistent with an MHD model in which the kinetic energy of the expansion is transformed into random electron motion [15]. Simultaneously, the plasma expands slowly along the magnetic field. This may be the reason behind the observed intensity decrease. The decreased intensity may be going right to some other emissions. The intensity enhancements in some previous reports may be due to this.

Electron-impact collisions are supposed to be the dominant process producing excited species in expanding plume. In other words, we could say that any change in electron density affects the observed intensity of an emission line. Since the presence of magnetic field largely deviates the expansion direction of electrons (because of their low mass), the reduction in intensity is also attributed to the deficiency of electrons in the observable volume [16] at the entrance slit of spectrometer.

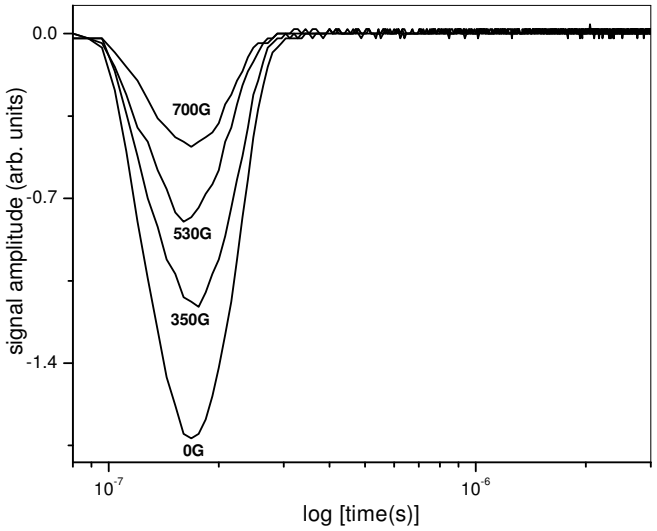


Fig 4. 8: Temporal profile of Li II (5484Å) with magnetic field in diffusion vacuum. laser energy is 140mJ.

Harilal et al. [15] also observed a considerable reduction in intensity for the neutral and singly ionized Al plasma species and an enhanced emission from multiply charged Al ions in a transverse magnetic field. Their conclusion is that the relative rise in intensity of transitions involving higher levels is mainly due to rise in the mean electron energy in the plasma. This also suggests that the intensity of recombination radiation is strongly reduced by the field. Rai *et al.* [17] attributed the reduction in emission intensity in the presence of a magnetic field to loss of plasma energy, which may be due to the opening of a new channel of loss in the content of plasma energy. The generation of

instabilities and high-energy particles in the plasma along with self-absorption of emissions by the plasma may be the reason for the loss of plasma energy.

Both the neutral and singly ionized species are showing the same delay, with and without the presence of magnetic field. This means that magnetic field does not much affect the arrival time distribution of the ejected species.

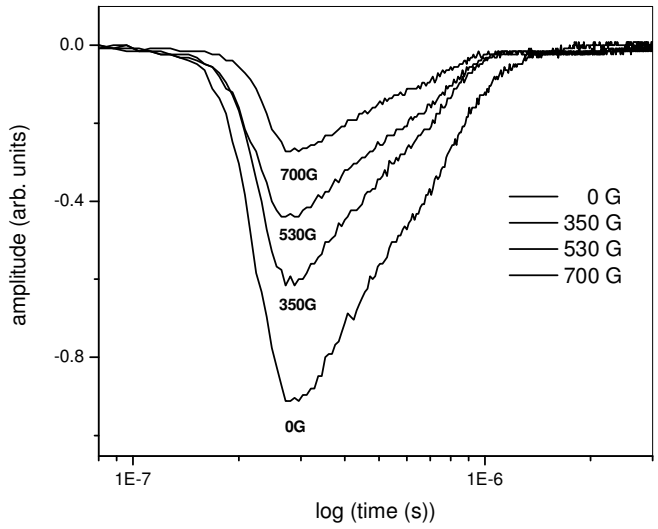


*Fig 4. 9: Temporal profile of Li I (6103Å) with magnetic field in diffusion vacuum and at laser energy of 140mJ.*

### 4.5.2. Effect of magnetic field on LIP in argon ambient

The ambient gas greatly influences the temporal profiles of the expanding plume. The slow components appear strongly at 6mm distance. As the neutrals are one of the major constituent species in the plume and ambient gas is the prime source responsible for excitation/ionization of neutral atoms. The increase in emission intensity of expanding plume in background gas is mainly due to two processes: (i) excitations due to collisions with background atoms and (ii) electron impact excitation. Of these two cases, electron impact processes plays the dominant role in the enhancement of the excited species in expanding plasma [18, 19]. The interaction between the expanding plasma and ambient gas causes the ionization of

buffer gas resulting in production of more number of free electrons. The enhanced electron density leads to increase in excitations of species [20].

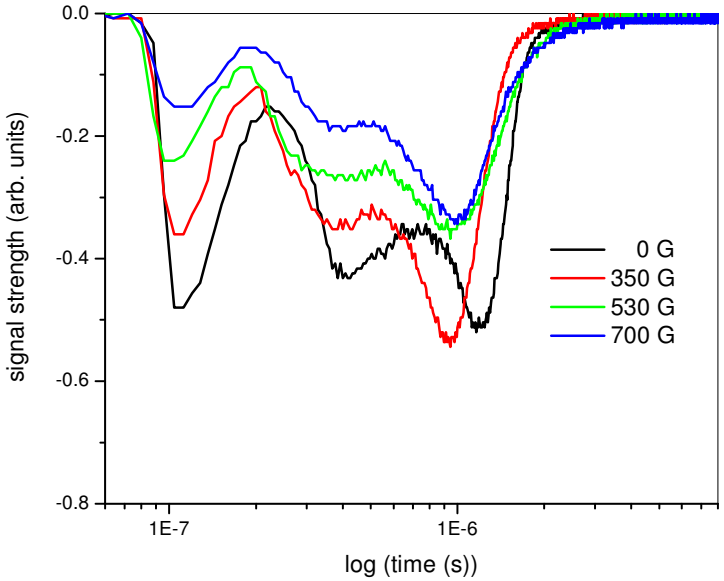


Fig 4.10: Multiple peak structure of LiI (6708Å) in magnetic field at 1mbar pressure. Laser energy is 140mJ.

With ambient argon (1mbar), the neutral profiles show both double peak and triple peak behaviour. Each component of the multiple peak structures shows independent response to the applied field. The plasma is more electron rich, as the argon-excited states are also abundant. It has been shown that plasma formed in argon atmosphere is hotter and denser compared to air as the ambient [21]. Here there is more probability that different fractions of the respective emitting species (neutral or charged) will be of a different origin and therefore different time scales will be involved in the emission, when we look upon the time profile of a specific emission at a definite wavelength. The response of the peak structures are seen in the results presented in figures 4.10 and 4.11.

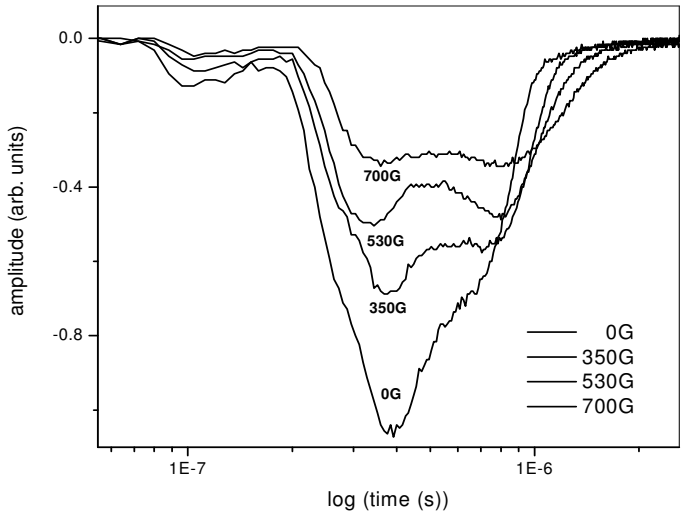


Fig 4.11: Multiple peak structure of LiI (6103Å) in magnetic field at 1mbar pressure. Laser energy is 140mJ.

### 4.5.3. Splitting of neutral line profiles

Excited neutral species are sustained for a longer time in the plume compared to the singly ionized species (figures 4.8 and 4.9). i.e., neutral profiles are much broader than those of ionic species. This suggests that the effects of magnetic field are more on neutral species. This is because the major constituent of the plume is neutrals and the excitation source is the electron impact collision processes. So, any deviation in the electron density could be reflected on the observed emission intensity of neutral species also.

The temporal profiles of neutral plasma species in the field show a splitting. Formation of an additional peak in the line profile of neutral species (6708Å) is the result of a plume splitting in the field. For the neutral line at 6708 Å in vacuum, this new peak has been recorded 1μs after the original emission. An earlier appearance of the second peak is found in ambient argon at 1mb. This can be seen in the time profile of Li I (6103Å) in the plasma produced by irradiating the target with 140mJ of laser energy (Fig.4.11) over a spot of diameter 1mm.

In addition to those formed from the laser excitation, neutrals are also produced by recombination processes:

$$A^+ + e^- \rightarrow A \qquad (4.12)$$

The electrons in the plume are effectively magnetized by the magnetic field lines than the ions. However, the inhomogeneous space-charge which results from this generates an electric field in a direction perpendicular to the laser spot axis, which will attract the ions towards the central axis of the plume. In effect, a progressive drift of charges takes place and the magnetic field will indirectly confine the ions as well as the electrons [22, 23]. It is expected that fast electrons and ions travel at the leading edge of the plasma. After the laser action ceases, the charge composition of the plasma is governed by three body recombination, which dominates over radiative and electronic effects due to the rapid drop in electron temperature as the plasma expands. The ions located at the front of the plasma acquire the largest energy during hydrodynamic acceleration and their interaction time for recombination is very much reduced [24]. Thus, the recombination are delayed and this may be the reason for a delayed peak (Fig. 4.12). This is found to exist at distances greater than 6mm. Another possible effect for the existence of delayed peak with neutrals is the back flow of the particles towards the target, after the collapse of diamagnetic cavity of the plasma.

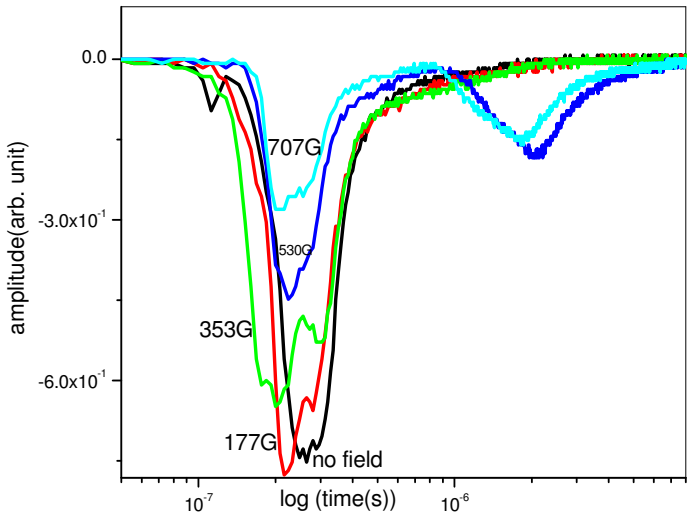


Fig 4.12: Vacuum profile of Li I (6708Å)in magnetic field at laser energy of 140mJ.

## 4.6. Summary

The main objective of the experiments presented here is to investigate the behaviour of LIP under the influence of a perpendicular magnetic field. The plume is

created using a ns laser pulse hitting a lithium rod in vacuum and argon ambient environments. The pulsed magnetic field applied to plasma has been created using a Helmholtz coil. The plasma is examined using spectroscopic measurements and found that the magnetic field does not much affect the arrival time distribution of the ejected species but the intensity of visible radiation is modulated by the field. Neutrals are greatly affected by the modified collisions and recombination behavior.

## 4.7. References

[1] Ira B. Bernstein, Phys. Rev. 109 10 (1958)

[2] Linlor W I, Appl Phys Lett 3 210 (1963)

[3]William I. Linlor, Phy Rev lett 12 383 (1964)

[4]M Mattioli and D Veron, Plasma Phys 11 684 (1969)

[5] Haught A F, Polk D H and Fader W J, Phys Fluids 13 2842 (1970)

[6] Tuckfield R G and Schwirzke F, Plasma Phys 11 11 (1969)

[7] Sucov E W, Pack J L, Phelps A V and Engelhardt A G, Phys Fluids 10 2035 (1967)

[8] F F Chen, Introduction to plasma physics (Plenum, New york, 1974)

[9] V N Rai, M Shukla and H C Pant, Pramana, J Phys 52 49 (1999)

[10] T. A. Peyser, C. K. Manka, B. H. Ripin, and G. Ganguli, Phys Fluids B 4 2448 (1992)

[11] B. H. Ripin, J. D. Huba, E. A. McLean, C. K. Manka, T. Peyser, H. R. Burris and J. Grun, Phys Fluids B 5 3491 (1993)

[12] M. VanZeeland, W. Gekelman, S. Vincena, and J. Maggs, Phys Plasmas 10 1243 (2003)

[13] A A Harms, K F Schoepf, G H Miley, Principles of Fusion Energy (World scientific, Singapore, 2000)

[14] J D Huba, N R L Plasma Formulary (Naval Research Laboratory, Washington D C, 2002)

[15] S. S. Harilal, M. S. Tillack, B. O'Shay, C. V. Bindhu, and F. Najmabadi, Physical Review E 69 026413 (2004)

[16] X. K. Shen, Y. F. Lu, T. Gebre, H. Ling and Y. X. Han, J Appl Phy 100 053303 (2006)

[17] V. N. Rai, J. P. Singh, F. Y. Yueh, R.L.Cook, *Laser and Particle Beams 21* 65 (2003)

[18] C. Timmer, S.K. Srivastava, T.E. Hall and A. Fucaloro, J. Appl. Phys. 70 1888 (1991)

[19] H. P. Gu, Q.H. Lou, N.H. Cheung, S.C. Chen, Z. Y. Wang and P.K. Liu, Appl. Phys. B 58 143 (1994)

[20] J. Gonzalo, F. Vega and C.N. Afonso, J. Appl. Phys. 77 6588 (1995)

[21] S. S. Harilal, C. V. Bindhu, V. P. N. Nampoori and C. P. G. Vallabhan, Appl Phys Lett 72(2) 167 (1998)

[22] A Anders, S Anders and I Brown, J Appl Phys 75 (10) 4900 (1994)

[23] R Jordan and J Lunney, Appl Surf. Sci.109/110 403 (1997)

[24] S. S. Harilal, C. V. Bindhu, M. S. Tillack, F. Najmabadi and A. C. Gaeris, J Appl Phys. 93 2380 (2003)